Influence of the number of dynamic analyses on the accuracy of structural response estimates

Pierre Gehl, John Douglas, Darius Seyedi

Influence of the Number of Dynamic Analyses on the Accuracy of Structural Response Estimates

Pierre Gehl,[a] John Douglas,[a] and Darius M. Seyedi[a), b]

Nonlinear dynamic analysis is often used to develop fragility curves within the framework of seismic risk assessment and performance-based earthquake engineering. In the present article, fragility curves are derived from randomly generated clouds of structural response results by using least squares and sum-of-squares regression, and maximum likelihood estimation. Different statistical measures are used to estimate the quality of fragility functions derived by considering varying numbers of ground motions. Graphs are proposed that can be used as guidance regarding the number of calculations required for these three approaches. The effectiveness of the results is demonstrated by their application to a structural model. The results show that the least-squares method for deriving fragility functions converges much faster than the maximum likelihood and sum-of-squares approaches. With the least-squares approach, a few dozen records might be sufficient to obtain satisfactory estimates, whereas using the maximum likelihood approach may require several times more calculations to attain the same accuracy. [DOI: 10.1193/102912EQS320M]

INTRODUCTION

Fragility curves assess the probability that a structural system suffers a certain damage level given an assumed level of earthquake shaking, characterized by an intensity measure (IM), such as peak ground acceleration or spectral acceleration at a period of interest. By providing the link between the seismic hazard and the structure's damage state (DS), through the study of the structural response represented by an engineering demand parameter (EDP), fragility curves represent a basis for the majority of modern earthquake risk assessments as well as performance-based earthquake engineering. Consequently, many such curves have been proposed for various structural types and IMs. The various methods of fragility evaluation can be divided into two primary categories (Calvi et al. 2006): empirical, based on the damage observed after earthquakes, and analytical. In analytical methods, damage distributions are simulated through the analysis of structural models, generally by using the static pushover method [Applied Technology Council (*ATC*)-*40* 1996] or dynamic nonlinear analysis.

The paucity of accelerograms for all earthquake scenarios of interest and the relatively high cost of nonlinear dynamic calculations encourage the use of a minimal but sufficient number of ground motions for deriving fragility curves. Incremental dynamic analysis (IDA)

[a] BRGM – DRP, 3 avenue C. Guillemin, BP36009, 45060 Orleans Cedex 2, France
[b] Now at: ANDRA – R&D, 1/7, rue Jean Monnet, 92298 Châtenay-Malabry Cedex, France

Earthquake Spectra, Volume 31, No. 1, pages 97–113, February 2015;

intends to overcome the first problem (Vamvatsikos and Cornell 2002). In IDA, a structural model is subjected to a series of ground motion records, each scaled to various levels of intensity. In this way, several records are produced by progressively increasing the ground motion amplitudes, without modifying their spectral shapes, to obtain a sufficient number of records. The primary concern is whether the damage states obtained from scaled records accurately estimate those obtained from unscaled ones. It has been shown that the scatter of structural response depends on the selected IM, which depends on the studied structure (Bommer et al. 2004, Gehl et al. 2013). Thus, the accuracy of IDA will depend on the chosen IM, the type of structure, and the scaling approach [Vamvatsikos and Cornell 2002, Pacific Earthquake Engineering Research Center (PEER) 2009].

Currently, there is little guidance in the literature regarding how many dynamic runs (time-histories) need to be used to obtain robust fragility curves. Shome et al. (1998), Hancock et al. (2008), and more recently, Buratti et al. (2011) proposed that only a handful of well-chosen dynamic runs are required to accurately assess structural responses for a given earthquake scenario. Fragility curves seek to capture structural responses for all possible earthquake scenarios; therefore, it is likely that more time-histories are needed for their robust evaluation than proposed by these authors for a single scenario. However, as shown by Shome et al. (1998) for a five-story steel moment-resisting frame (and by others for different structures), after conditioning for response spectral acceleration, there is little dependence in structural response over a wider range of magnitude and distance (i.e., the IM is *sufficient*). The conjecture that many records are required to define fragility curves is supported by the amounts used by, for example, Shinozuka et al. (2000) and Karim and Yamazaki (2003) to develop fragility curves for bridges using 80 and 250 accelerograms, respectively. A recent study (Saez et al. 2011) highlights the importance of the number of ground motions used to provide fragility curves. The authors develop fragility curves by using the maximum likelihood method considering different numbers of nonscaled ground motions. Assuming a lognormal distribution for the fragility curves, the Fisher information matrix is used to measure the ability of the data, i.e., the accelerograms, to estimate the parameters of the curves. It is worth noting that the Fisher information matrix can only be used when the maximum likelihood method is employed.

Following an introduction to the derivation of fragility curves, this article provides guidance on the statistical confidence of fragility curves by randomly generating dozens of sets of structural response data from known fragility curves, then applying three commonly used approaches [regression techniques based on least squares (LS), maximum likelihood (MLE), and sum-of-squared errors (SSE) formulations] to derive fragility curves from these data, which can then be compared to the original curves. This procedure leads to graphs that can be used for guidance concerning how many calculations are required to obtain a certain accuracy level in the fragility curve. This guidance is verified against simulated damage, computed by using a single-degree-of-freedom (SDOF) model of nonlinear structural response. The article ends with some brief conclusions.

STRUCTURAL RESPONSE ESTIMATION FOR THE DERIVATION OF FRAGILITY CURVES

Using the PEER equation (Cornell and Krawinkler 2000) of the mean annual probability of exceeding a given $DS = ds$, the fragility of a structural system can be written as

$$P(DS \geq ds|IM) = \int P(DS \geq ds|EDP) \cdot \left| \frac{dP(EDP|IM)}{dedp} \right| \cdot dedp \tag{1}$$

where *EDP* represents the engineering demand parameter (e.g., interstory drift, local strain or stress, or accumulated energy in the structural system) and *IM* stands for the intensity measure of the seismic loading (e.g., elastic response spectral displacement or acceleration at a period of interest). Maximum interstory drift ratio is a widely used EDP because its computation through dynamic analyses is rather straightforward and the link with damage to the structure can be performed through empirical correlations. Therefore, the rest of the present study will assume drift as the EDP, although this EDP is not necessarily the most appropriate for all structure types and additional parameters, such as peak floor acceleration, are advocated by recent guidelines (e.g., *ATC-58* 2011). However, the conclusions drawn from the present study apply to the generic probabilistic relation between an IM and an EDP, regardless of their nature. The scope of this study is limited to the estimation of the structural response, i.e., the conditional probability of exceeding a given EDP level with respect to an IM. Indeed, there is a gap in the literature regarding the mapping between EDP and the resulting DS, which can only be filled through extensive experimentation and measurement campaigns (Moehle and Deierlein 2004). Therefore, most common approaches rely on the definition of a certain EDP threshold (i.e., the structural capacity, denoted C_{ds}) that will imply the occurrence of a DS. Certain studies propose a probabilistic relation between EDP and DS (e.g., a lognormal distribution) and its associated standard deviation; for instance, $\beta_{ds} = 0.4$, as suggested in the HAZUS framework (NIBS 2004). This approach has been adopted here. It is represented by the following equation:

$$P(DS \geq ds|EDP) = \Phi\left[\frac{\ln EDP - \ln C_{ds}}{\beta_{ds}}\right] \tag{2}$$

where Φ represents the normal cumulative distribution function and β_{ds} is established as equal to 0.4. Based on this assumption, a combination of Equations 1 and 2 yields the following expression of fragility:

$$P(DS \geq ds|IM) = \int \Phi\left[\frac{\ln EDP - \ln C_{ds}}{\beta_{ds}}\right] \cdot \left| \frac{dp(EDP|IM)}{dedp} \right| \cdot dedp \tag{3}$$

One widely used method for estimating the probabilistic relation between the parameters EDP and IM is to perform an LS regression on the results of dynamic analyses (Cornell et al. 2002, Ellingwood and Kinali 2009), assuming a lognormal distribution (Shome and Cornell 1999). The predicted demand parameter, $\widehat{EDP}$, is represented by a power law, with β_ε being the standard deviation of the error term of the logarithm of the predicted demand parameter (see Figure 1). Parallel developments have been made in the estimation of the parameters of fragility curves, based on MLE (Shinozuka et al. 2000), for which, as in the LS approach, a lognormal distribution is usually assumed. The median and standard deviation (α and β, respectively) of the lognormal distribution are then estimated through the maximization of a likelihood function (see Figure 1b). Finally, similarly to MLE, an approach based

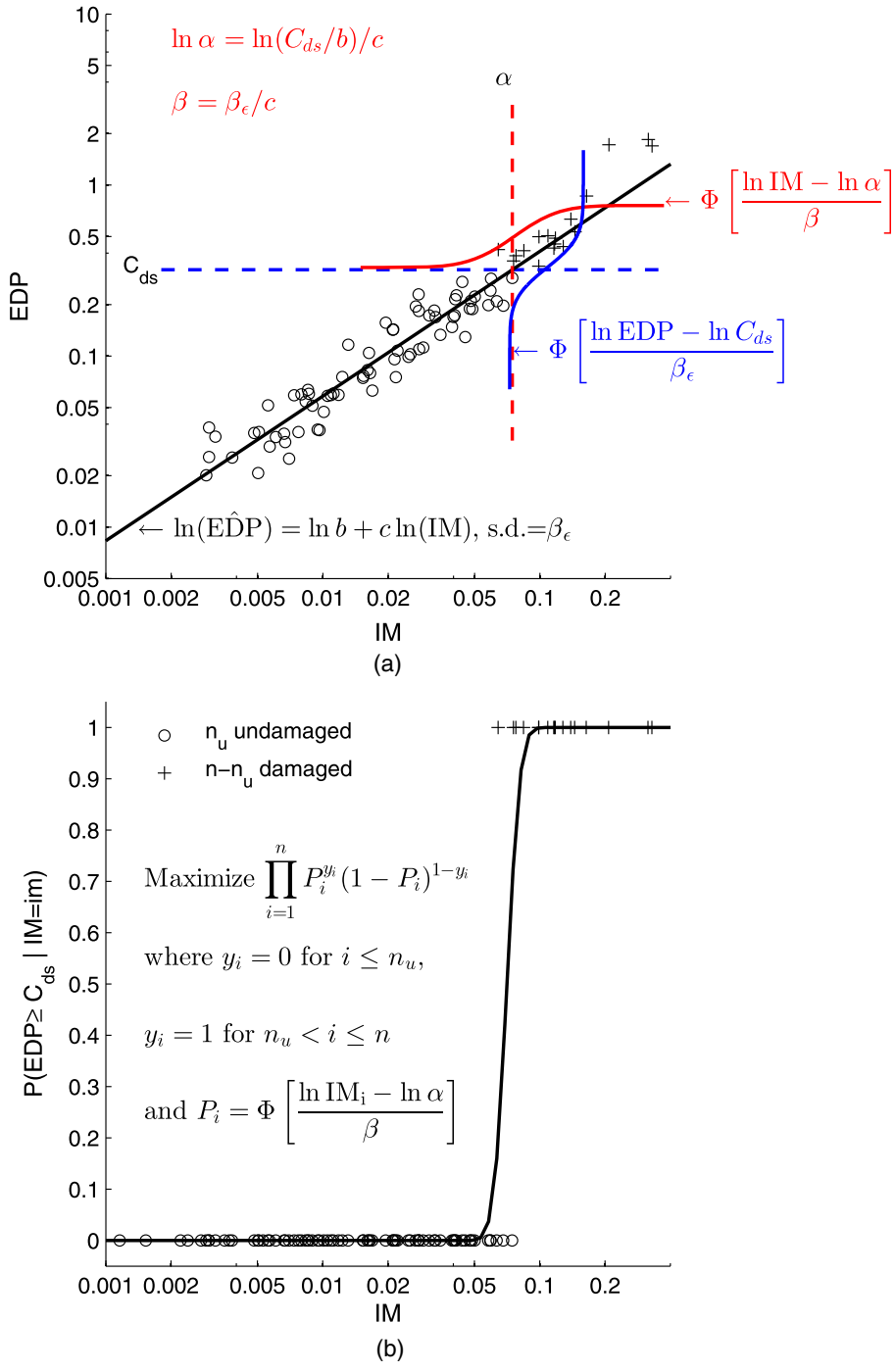

Figure 1. Schematic representation of the derivation of fragility curves by using the approaches under consideration: (a) least-squares regression and (b) maximum likelihood estimation when the damage threshold, C_{ds}, is assumed to be exactly known (i.e., $\beta_{ds} = 0$). Here, b and c are coefficients of the power law connecting the EDP to the IM and n is the number of calculations.

on SSE has been investigated by Baker (2013), where the function to minimize is defined as follows, using the same notations as in Figure 1:

$$L(\alpha, \beta) = \sum_{i=1}^{n} (y_i - P_i)^2 \tag{4}$$

The use of the lognormal assumption to represent the relation between EDP and IM enables the convolution of the two lognormal cumulative distribution functions. Equation 3 can consequently be rewritten as follows, with a global standard deviation $\beta_{tot} = \sqrt{\beta^2 + \beta_{ds}^2}$:

$$P(DS \geq ds|IM) = \Phi\left[\frac{\ln IM - \ln \alpha}{\sqrt{\beta^2 + \beta_{ds}^2}}\right] \tag{5}$$

MLE was originally used to develop fragility curves from empirical data, including post-earthquake observations of bridge damage (Shinozuka et al. 2000), because it requires only binary information (damage or no damage) and no drift calculations or estimates, which cannot be accurately obtained from post-earthquake field surveys (from which only residual drifts can be observed). Several studies have also used MLE to postprocess the results of nonlinear time-history analyses (Kim and Shinozuka 2004, Zentner 2010), directly switching from drift values to the corresponding binary outcomes in terms of damage states. The use of MLE in the latter context may seem counterproductive, because it results in the loss of information (i.e., the actual value of the computed drifts). This drawback, however, may change to an advantage when the development of near collapse or collapse fragility curves is considered (Baker 2013) because, in this case, most computation codes may return unreliable results or may not even converge, thus making LS regression difficult to apply (Shome and Cornell 2000). In addition, MLE does not assume a predefined relation between IM and EDP (e.g., a power law), unlike the LS approach, which may be useful in the case of poorly correlated or constrained dynamic results.

LS regression is an efficient way to establish a robust relation between EDP and IM with only a few data points, because it uses all information contained in the simulation results. It is also possible to extrapolate the regression line to higher or lower IM values when such levels are not covered by the time-history analyses, although extrapolation is generally not recommended because structural behavior may alter beyond the range covered by the available analyses. One drawback of this method is that the standard deviation, β_ε, of the error term is often computed over the whole IM range, resulting in the same dispersion in the fragility curves for various damage levels. However, this limitation can be avoided by performing piecewise regressions over different IM intervals (Carausu and Vulpe 1996), which allows the power law and dispersion to vary with the level of IM.

The review by Baker (2007) discussing ways to perform probabilistic structural response assessment provides a useful summary of the pros and cons of the different methods. Out of the several derivation techniques discussed by Baker (2007), only the so-called linear

regression on a cloud is tested here (i.e., that corresponding to LS regression); the other techniques covered by Baker (2007) may be viewed as more elaborate variants that rely mostly on the scaling of ground motion records, which is out of the scope of the present paper. Porter et al. (2007) also comprehensively review various techniques to derive fragility curves, focusing on those used for experimental results, among which the most similar to the LS regression evaluated here is designated method A. Other approaches reviewed by Porter et al. (2007) imply the use of expert judgment or the combination of both empirical and analytical data, which makes them difficult to apply in the present study.

TRIAL INVERSION PROCEDURE

To assess the reliability of fragility curves derived from a limited number of time-history analyses, we undertake a series of inversions on simulated data. This procedure enables comparison between the computed estimates and the true fragility parameters, thus constituting an efficient means to evaluate the robustness of the three regression techniques as a function of the number of data points (i.e., dynamic analyses). This inversion procedure is broken down into the following steps:

1. The initial fragility parameters, α_0 and β_0, are established, along with the corresponding relation: $\log \widehat{EDP} = \log b_0 + c_0 \cdot \log IM + \varepsilon$ $(\varepsilon \sim N[0, \beta_\varepsilon^2])$ and a probabilistic damage threshold, C_{ds}, is assumed. Therefore, the global standard deviation of the relation between the IM and the damage state can be written as:

$$\beta_{0,tot} = \sqrt{\beta_0^2 + \beta_{ds}^2}.$$

2. A set of n IM values are defined and the corresponding EDP values are sampled based on the relation in step 1 and the corresponding error term, ε. The n data points represent the n dynamic analyses that yield the pairs (IM, EDP). The IMs are assumed to be applicable for all magnitude (M) and distance (R), and consequently, should be considered for all possible earthquake scenarios and associated ground motions. Assuming uniform distributions of M and R and lognormal ground motion variability leads to IMs that are lognormally distributed (this has been numerically verified by using a large strong-motion database), which is assumed with sufficient standard deviation to cover the entire range of possible ground motions. The series of IMs are also chosen such that approximately half of the points are below the damage threshold (C_{ds}) and half above, which corresponds to the most favorable configuration for the estimation of parameters via MLE and SSE techniques. Therefore, the use of a lognormal distribution of the IMs, with a median corresponding to the damage threshold, represents the ideal case with the best use of the available data samples, as stressed by Kato et al. (2008) via their study of information entropy.
3. Using the n pairs of IM-EDP values, fragility curves are derived, as defined in Equation 5, by using the three regression techniques described in the previous section. The estimated fragility parameters $\hat{\alpha}$ and $\hat{\beta}_{tot} = \sqrt{\hat{\beta}^2 + \beta_{ds}^2}$ can then be compared to the "true" parameters, α_0 and $\beta_{0,tot}$.

4. Steps 2 and 3 are repeated k times ($k \gg 1$) to obtain stable estimates of the errors and confidence intervals of the estimated fragility parameters.

Using the set of k fragility estimates, several metrics are computed to obtain objective measures of the accuracy of fragility functions with respect to the number of data points. Intuitive indicators are the standard deviations of both $\hat{\alpha}$ and $\hat{\beta}$, which can be computed for k pairs using a bootstrap technique (Efron and Tibshirani 1993).

By using the inversion procedure, the fragility parameters obtained from the simulated data points can also be compared to the original parameters, α_0 and β_0. Therefore, this feature can provide valuable information on the accuracy of the fragility estimates, and not only their precision. The accuracy of an estimate can be quantified by how close it is to the true value, whereas its precision represents only the narrowness of the confidence intervals (i.e., standard deviation of the estimate), with no information about the level of bias. Thus, to compare two fragility curves, the Kolmogorov-Smirnov statistic, D, has been chosen to measure the largest absolute difference between the original and estimated lognormal distributions. This D metric provides an adequate measure of the maximum bias induced by different curves and can be viewed as an indicator of the accuracy of the fragility curve. However, the use of D may induce a bias in the interpretation of results, particularly when addressing low probabilities. A normalized D may be used as a metric measuring the difference between two curves because this would give more weight to discrepancies between the curves at low probabilities, which may be relatively more important than differences at the upper end of the curves. However, because the calculation of normalized D requires division by the theoretical (lognormal) distribution, it can overemphasize the lower tail of the distribution, which may not satisfactorily describe the real damage distribution (Kennedy et al. 1980); additionally, the midrange of the fragility curve is generally the most important when, for example, computing the collapse risk (Eads et al. 2013).

RESULTS AND IMPLICATIONS

The trial inversion procedure introduced above is conducted with $k = 10{,}000$ to obtain stable statistics. The following robustness indicators are computed for various numbers of data points (n ranging from 20 to 500) and for each of the three techniques (LS, MLE, and SSE):

- Coefficients of variation (COVs, standard deviation divided by the mean) of the parameters $\hat{\alpha}$ and $\hat{\beta}$, to measure the precision of these terms.
- Mean of the Kolmogorov-Smirnov distance, D, over all k simulations, to compare the initial true distribution with that estimated.

These results are presented in a series of graphs (see Figure 2) to show the evolution of each indicator with respect to the number of dynamic analyses. For the LS approach, it is possible (Draper and Smith 1981) to explicitly express the standard deviation of the terms $\ln b$ and c in the regression equation, based on the numbers of samples (i.e., n), the standard deviation of the regression, and the distribution of the input variable (i.e., IM). Therefore, an analytical estimation of the standard deviations of $\ln b$ and c has been performed and the COVs of α and β have been evaluated by using an error propagation procedure (Ku 1966). It is found that the analytical results are within 5% of the values obtained from the numerical

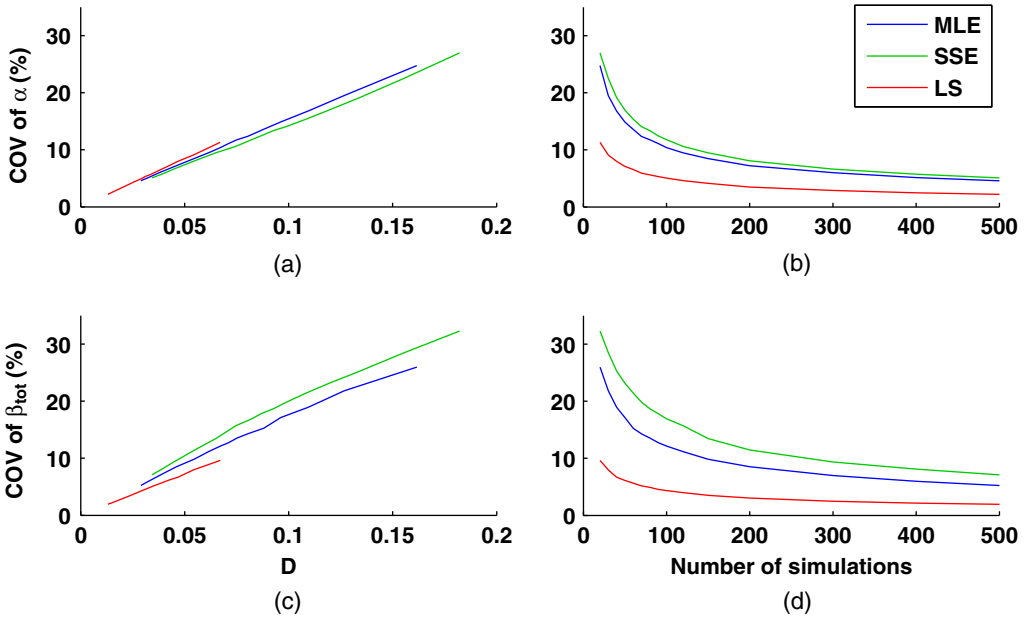

Figure 2. (a) Correspondence between the uncertainty on the fragility median, α, and the D metric; (b) evolution of the uncertainty on α with the number of simulations; (c), (d) same construction for the fragility standard deviation, β_{tot}. The results from the three regression techniques (MLE, SSE, and LS, respectively) are plotted in blue, green, and red.

approach, thus validating the results from the inversion procedure (see Appendix A). These analytical estimations are valuable for verifying the dispersion of the coefficients of the fragility curve (i.e., their precision), but they are not able to predict the accuracy of the curve, for which the Monte Carlo approach is required.

Figure 2 constitutes objective guidance regarding how many simulations are required for a given objective (value of D) and the derivation technique that is used. For example, if it is decided that the fragility curve inaccuracy should not exceed $D = 0.05$ (error of 5%), then this goal implies that the coefficient of variation of α should not exceed 8.4% (top left graph), thus requiring approximately 40 simulations for processing by using least-squares regression (top right graph). These results show also the poor performance of the MLE and SSE approaches, which require between 150 and 300 runs to attain the same level of accuracy. This observation was to be expected, because MLE and SSE approaches rely on binary outcomes and require less information than the LS regression (which directly uses EDP values). These methods, however, still present other advantages, as explained above (e.g., in the case of nonconvergence of dynamic runs, when considering collapse, or when analyzing post-earthquake observations).

The number of simulations required for the ML approach, according to Figure 2, may seem large at first glance because it is higher than the number of records usually used in previous studies (Shinozuka et al. 2000). However, using the D metric as a measure of the

Table 1. Results from the inversion procedure, providing the link between the number of data points, the COV of α and β, and the Kolmogorov-Smirnov distance, D, for the three derivation techniques

No. of simulations	COV of α (%)			COV of β_{tot} (%)			D		
	MLE	SSE	LS	MLE	SSE	LS	MLE	SSE	LS
20	24.7	27.0	11.3	26.0	32.3	9.6	0.162	0.182	0.067
30	19.5	22.5	9.1	21.8	28.5	8.0	0.127	0.156	0.054
40	16.8	19.2	8.0	18.9	25.3	6.7	0.110	0.134	0.047
50	14.9	17.0	7.1	17.1	23.2	6.1	0.096	0.120	0.042
80	11.8	13.4	5.6	13.5	18.7	4.9	0.075	0.093	0.033
100	10.4	11.8	5.1	12.1	16.9	4.3	0.067	0.082	0.030
150	8.5	9.5	4.1	9.8	13.5	3.5	0.055	0.065	0.024
200	7.2	8.1	3.5	8.5	11.5	3.0	0.046	0.055	0.021
300	6.0	6.6	2.9	7.0	9.4	2.5	0.038	0.045	0.017
400	5.1	5.7	2.5	6.0	8.1	2.1	0.033	0.039	0.015
500	4.6	5.1	2.2	5.2	7.1	1.9	0.029	0.034	0.013

accuracy of the resulting parameters, it can be shown that even with a limited number of simulations (i.e., under 100), the derived curves would still be contained within an error range of approximately 10%. Figure 2 provides a link between the precision and accuracy of the results: whereas the precision of the fragility parameters (i.e., narrow confidence bounds) can be obtained by using a straightforward bootstrap procedure, consequences on the accuracy of the results, which are usually inaccessible without the knowledge of the true distribution, can be approximated by the empirical relations provided in Figure 2a. As a result, based on Figure 2, numerical results from the trial inversion procedure are presented in Table 1 to provide guidance on the level of performance that can be expected for future fragility derivation studies, depending on the regression technique and the number of data points.

The introduction of additional uncertainty in the definition of DS (i.e., β_{ds}) puts into perspective the effect of the record-to-record variability, which is the focus here. Indeed, there is little point in trying to obtain a perfect estimate of the structural response with respect to an IM, because other sources of variability, such as the damage state definition or modeling uncertainties, may be higher still and tend to dilute the effect of the variability due to the seismic input. The uncertainties related to structural response calculation may be reduced by using more accurate structural models, particularly when addressing a particular structure, whereas the record-to-record variability is related to the random nature of earthquake hazard.

The results from Table 1 have been computed by selecting an initial standard deviation, $\beta_0 = 0.5$, which lies within the common range of dispersion for most fragility curves (e.g., standard deviations proposed within HAZUS; NIBS 2004). A sensitivity study has also been conducted to verify the effect of the standard deviation on the number of required simulations

(see Table 2 and Figure 3). The calculations are performed for a range of β_0 and three values of β_{ds}. The following observations can be noted:

- For the three techniques, the value of β_{ds} has no effect on the precision of α, which decreases (i.e., the estimate is associated with a higher standard deviation) roughly linearly as β_0 increases.
- For the least-squares approach, the precision of β_{tot} is roughly unchanged by β_0 and β_{ds}, although it decreases slightly (i.e., higher COV) as β_0 increases for nonzero β_{ds}; whereas for the other two approaches, the precision of β_{tot} decreases (i.e., higher COV) to a peak and then increases (i.e., lower COV) for nonzero β_{ds}. However, when $\beta_{ds} = 0$, the precision of β_{tot} increases for increasing β_0 (the reason for

Table 2. Evolution of inversion results with the value of the initial standard deviation, β_0, for three sizes of data sets (50, 100, and 200 simulations)

No. of simulations	Value of β_0	COV of α (%)			COV of β_{tot} (%)			D		
		MLE	SSE	LS	MLE	SSE	LS	MLE	SSE	LS
20	0.1	10.4	11.3	2.2	3.1	5.4	0.9	0.083	0.082	0.018
	0.5	24.5	26.8	11.3	25.7	31.5	9.9	0.163	0.184	0.067
	1	—	45.4	24.5	—	46.0	13.9	—	0.202	0.085
30	0.1	8.2	9.2	1.8	2.9	4.6	0.8	0.056	0.076	0.014
	0.5	19.1	21.7	9.4	21.6	28.1	7.8	0.126	0.152	0.055
	1	31.4	34.5	19.0	30.7	39.2	11.2	0.130	0.160	0.069
40	0.1	8.5	7.5	1.6	2.8	3.9	0.7	0.062	0.062	0.013
	0.5	17.2	19.5	8.0	19.1	25.3	6.7	0.112	0.137	0.047
	1	26.2	28.9	16.3	24.9	32.4	9.7	0.110	0.135	0.059
50	0.1	6.6	6.5	1.4	2.8	3.8	0.6	0.051	0.055	0.011
	0.5	14.8	16.8	7.1	17.0	23.2	6.2	0.096	0.119	0.042
	1	23.2	25.3	14.5	22.7	29.5	8.6	0.097	0.118	0.052
100	0.1	4.5	5.1	1.0	2.2	2.9	0.4	0.036	0.041	0.008
	0.5	10.5	11.6	5.0	12.0	16.9	4.3	0.067	0.081	0.030
	1	16.2	17.5	10.2	15.3	19.3	6.2	0.068	0.078	0.037
200	0.1	3.2	3.6	0.7	1.6	2.3	0.3	0.026	0.030	0.006
	0.5	7.3	8.1	3.6	8.5	11.6	3.1	0.047	0.056	0.021
	1	11.3	12.1	7.2	11.0	13.4	4.3	0.048	0.054	0.026

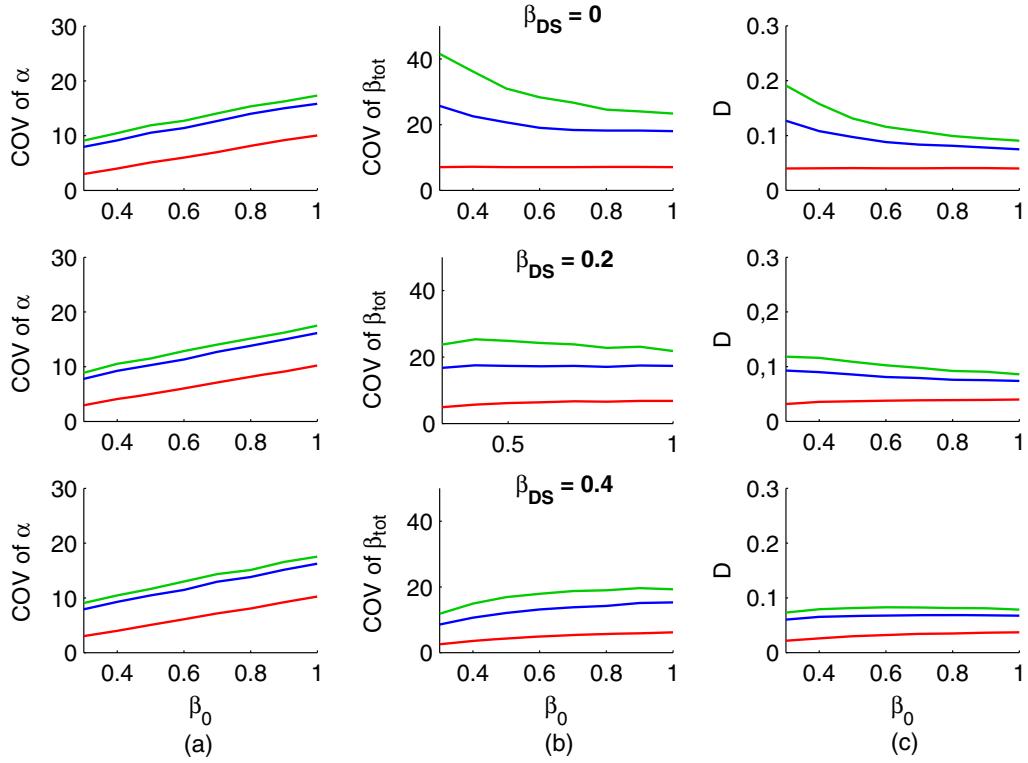

Figure 3. (a) Evolution of the COV of α with the value of β_0 for the three regression techniques (i.e., MLE in blue, SSE in green, and LS in red) and for a sample size of 100 simulations; (b) evolution of the COV of β_{tot} with the value of β_0 for the three regression techniques and for a sample size of 100 simulations; (c) evolution of D with the value of β_0 for the three regression techniques and for a sample size of 100 simulations.

this behavior is the interaction between the standard deviation of β_{tot} and the value of β_{tot}, which equals $\sqrt{\beta_0^2 + \beta_{ds}^2}$).

- Because of the strong influence of the precision of β_{tot} on the overall accuracy of the fragility curve, the dependence of D on changes in β_0 and β_{ds} is similar to the behavior of the curves for COV of β_{tot}; i.e., insignificant impact of β_0 and β_{ds} on the accuracy when using LS, and generally increasing accuracy as β_0 increases when using the other two approaches.

APPLICATION TO A SIMPLE STRUCTURAL MODEL

In this section, the previously discussed findings are compared to results obtained by considering the nonlinear structural response of an SDOF model. The modified Takeda model (Takeda et al. 1970) for reinforced concrete, which has been widely studied by Schwab and Lestuzzi (2007) and Lestuzzi et al. (2007), is used in this study because its robustness and low computational demand allow for a very large number of dynamic

Table 3. Parameters of the modified Takeda model of the studied structure

Parameter	Assigned value
Yield displacement	0.002 m
Post-yield stiffness ratio	5%
Coefficient of stiffness degradation	0.4
Target for reloading curve	0.0
Reduction factor	2
Viscous damping ratio	5%

analyses. The modified version of the model, initially developed by Takeda et al. (1970), is proposed by Otani (1974) and Litton (1975). The Takeda bilinear model includes many features to accurately mimic the behavior of reinforced concrete, such as a parameter governing stiffness degradation attributable to increasing damage and another for the reloading curve. Three other parameters are used to specify the behavior; namely, the initial (i.e., undamaged) stiffness, the yield displacement, and the post-yield stiffness ratio. The model does not account for strength degradation. A fundamental period of 0.5 s is chosen for this structure, corresponding roughly to a five-story (medium rise) building. Standard values are assigned to the parameters describing the model (see Table 3).

To obtain a reference fragility curve—that is a true distribution—the first step consists of submitting the structure to a very large number of records. Because there are insufficient natural ground motions in existing strong-motion databases, a set of synthetic ground motions was generated by using the nonstationary stochastic procedure proposed by Pousse et al. (2006). These signals have been generated for magnitudes (M_w) between 5.5 and 7.5 and epicentral distances between 10 and 100 km. The five Eurocode 8 soil classes are also sampled to introduce additional variability in the ground motion input. Approximately 100,000 of these records are generated and applied to the simplified model to obtain a well-constrained estimate of the structural response and its distribution. It is found that the IMs of the generated ground motions follow a lognormal distribution, as assumed earlier for the inversion. An arbitrary drift threshold is assumed so that approximately half of the simulations are below and the other half above (i.e., $C_{ds} = 0.16\%$ for drift ratio, which does not necessarily correspond to any particular damage state).

Using the LS regression approach, the large number of simulations allows confidence in the estimated fragility parameters (i.e., probability of exceeding the threshold C_{ds} given the IM, assumed as PSA at 0.5 s): $\alpha_{0,\mathrm{LS}} = 1.962\,\mathrm{m/s^2}$ and $\beta_{0,\mathrm{LS}} = 0.400$. However, the cloud graph between PSA (0.5 s) and the drift shows that the dispersion in the relation $EDP = f(IM)$ is not constant over the full range of IM (see Figure 4). Therefore, this configuration is slightly less ideal than that used in the inversion procedure above, and may lead to some bias. Thus, these parameters are still considered to be true (i.e., the reference fragility curve), but only for the LS regression approach. Using MLE and SSE, two different sets of true fragility parameters are also estimated using all simulation results; the results are $\alpha_{0,\mathrm{MLE}} = 1.846\,\mathrm{m/s^2}$ and $\beta_{0,\mathrm{MLE}} = 0.418$, and $\alpha_{0,\mathrm{SSE}} = 1.863\,\mathrm{m/s^2}$ and $\beta_{0,\mathrm{SSE}} = 0.400$,

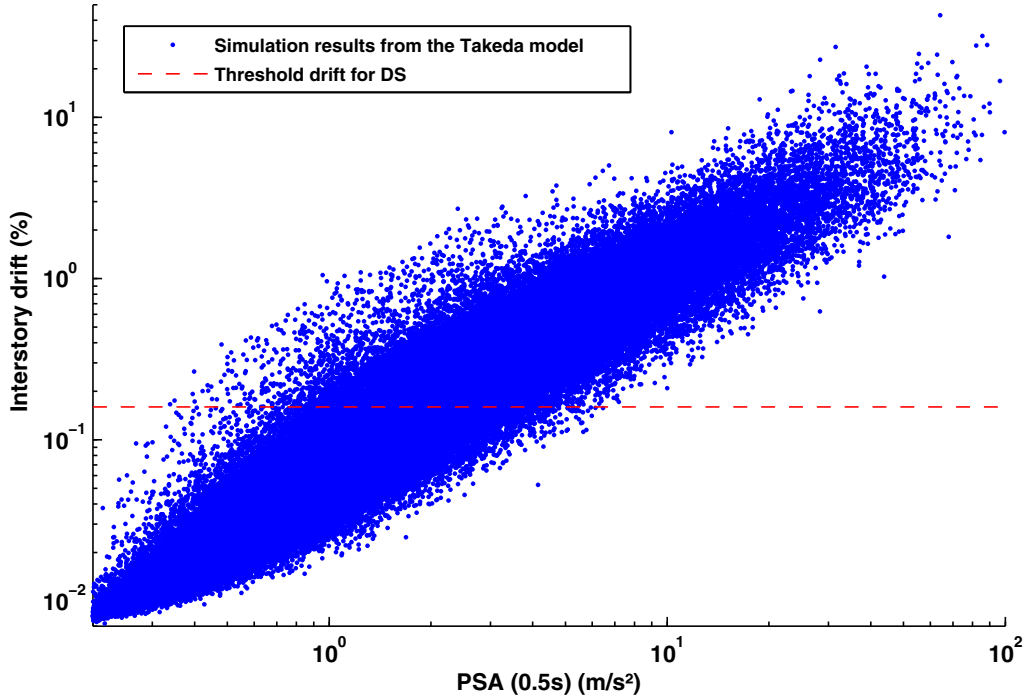

Figure 4. Correlation between the 100,000 drift values from the Takeda model and the chosen IM [PSA (0.5 s)].

respectively. These parameters are the basis of comparison for the successive fragility estimates, for both the MLE and SSE techniques.

The series of 100,000 simulation results is used to randomly select subsets of IM–EDP couples, their sizes ranging from 100 to 1,000. For each subset size, 10,000 samplings with replacement are conducted (i.e., a bootstrapping technique) to obtain stable statistics about the estimates of fragility parameters. The different metrics described in the previous section are then computed to measure the performance of the different fragility derivation approaches (LS, MLE, and SSE) for the different sample sizes and to verify whether the results obtained with this structural model confirm the generic findings from the trial inversion procedure. To remain consistent with the issue of dependence on the value of β_0, the results are compared with those of the inversion procedure conducted for $\beta_0 = 0.4$ (see Figure 5). Finally, the computed series of β, as well as the initial β_0, are combined with $\beta_{ds} = 0.4$ to account for the uncertainty attributable to the definition of damage state.

As shown in Figure 5, all metrics vary with the number of simulations in accordance with the theoretical inversion. In the case of the LS regression approach, satisfactory agreement with the theoretical findings is found and the metrics estimated through the inversion procedure are still slightly better than those obtained from the numerical model. This observation correlates with the assumption that the inversion procedure is based on a true power law with

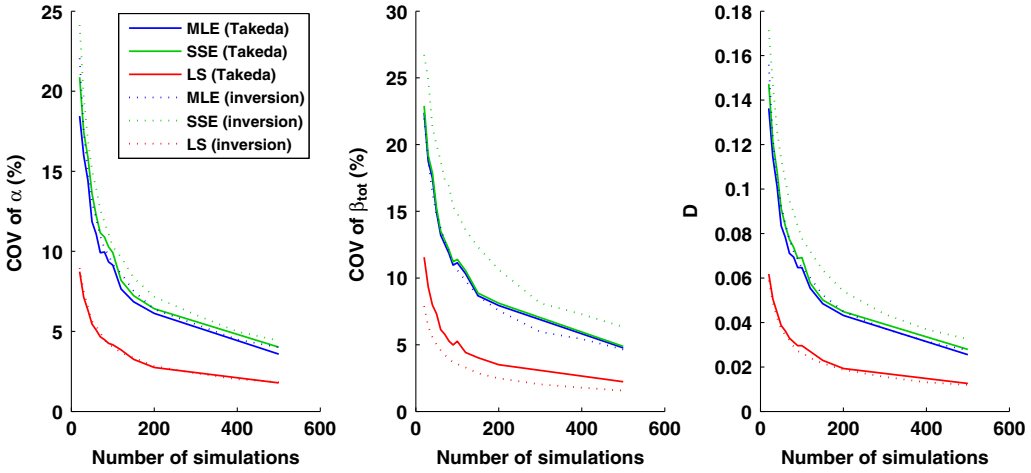

Figure 5. Comparison of the evolution of the metrics under consideration with the number of simulations, between the theoretical inversion (solid line) and the Takeda model application (dotted line).

constant dispersion, thus representing the ideal case. On the other hand, for the SSE method, the application results are slightly less consistent with the theoretical results, although still quite similar. The reason for this slight discrepancy is thought to be because of the nonlinear relation between the IM and drift, and also because of the nonuniform dispersion (Figure 4), in contrast to the assumptions made when developing the theoretical results. Moreover, the assumed threshold for the drift does not split all results into exactly two equivalent sets (above and below the threshold), which is the ideal case for the MLE and SSE techniques.

Whereas the choice of an SDOF model to perform this application may initially appear overly simple, it results from the observation that the conclusions from the inversion procedure are drawn from a basic statistical analysis of the relation between two parameters (i.e., EDP and IM) with no consideration of specific structural modeling. Therefore, these results are applicable to any type of structure, whether an SDOF or a more elaborate multiple-degree-of-freedom (MDOF) model, provided that the computed EDP can be expressed as a power law with respect to the IM. The huge number of runs required to generate an estimate of the true distribution (i.e., approximately 100,000, as explained above) prevents the use of an MDOF model for this validation example.

CONCLUSIONS

Generally, the LS regression method is preferred for the derivation of fragility curves because it requires far fewer time-histories to obtain an accurate fragility curve than the MLE and the SSE approaches. The MLE and SSE methods converge more slowly than the LS method when the derived fragility curves are compared with a true reference curve. However, MLE is recommended when drifts are unknown or inaccurate (e.g., for deriving collapse probabilities or when following earthquakes, observations are made of damaged/undamaged buildings). The use of the inversion procedure has allowed the

comparison of the estimated fragility parameters with the true parameters, thus providing valuable information that could not be reached by simply studying the convergence of the estimated parameters (i.e., confidence bounds evaluated through bootstrapping, for instance). For this reason, the use of such an inversion technique is preferable to the bootstrap approach, although it requires knowledge of the true model, which is generally not the case. The joint study of the precision and accuracy levels enables the proposal of relations between the coefficient of variation of the fragility parameters and the resulting error in terms of vulnerability assessment. Here, based on a trial inversion procedure and its validation through a simple case study, we provide guidance regarding the level of performance that can be expected, depending on the regression technique and the number of data points. The obtained results can be applied to any kind of structure if the computed EDP can be expressed as a power law with respect to the IM. However, the number of necessary calculations to obtain a given confidence level must be considered as an initial estimate because it is calculated for an idealized case. When considered in the context of performance-based earthquake engineering, this study has focused on the concerns related to the prediction of EDP given IM. The results indicate that a relatively small error is introduced into the final results by the limited number of analyses usually used. This can be easily corrected by performing more simulations. However, this is only one component in the risk assessment chain; other stages appear to contribute more to the overall uncertainty (e.g., prediction of damage state given EDP). These stages should receive more attention in the future.

ACKNOWLEDGMENTS

The work presented here was performed in the framework of the "Multi-Risks and Vulnerability" research program of BRGM, including the EDF/BRGM-funded MARS project, the ANR-funded EVSIM project, and the FP7-funded PERPETUATE project. We thank Jack Baker for sending us his recent paper on fitting fragility curves. The authors are very grateful to Prof. Peter Stafford for his constructive comments on an earlier version of this work and three anonymous reviewers for their detailed reviews of this article, which significantly improved the study.

REFERENCES

Applied Technology Council (ATC), 1996. *Seismic Evaluation and Retrofit of Concrete Buildings*, *Report No. ATC-40*, Redwood City, CA.

Applied Technology Council (ATC), 2011. *Seismic Performance Assessment of Buildings*, *Report No. ATC-58*, Redwood City, CA.

Baker, J., 2007. Probabilistic structural response assessment using vector-valued intensity measures, *Earthquake Engineering and Structural Dynamics* **36**, 1861–1883.

Baker, J. W., 2013. Efficient analytical fragility function fitting using dynamic structural analysis, *Earthquake Spectra* **31**, 579–599.

Bommer, J. J., Magenes, G., Hancock, J., and Penazzo, P., 2004. The influence of strong-motion duration on the seismic response of masonry structures, *Bulletin of Earthquake Engineering* **2**, 1–26.

Buratti, N., Stafford, P. J., and Bommer, J. J., 2011. Earthquake accelerogram selection and scaling procedures for estimating the distribution of drift response, *Journal of Structural Engineering* **137**, 345–357.

Calvi, G. M., Pinho, R., Magenes, G., Bommer, J. J., Restrepo-Velez, L. F., and Crowley, H., 2006. Development of seismic vulnerability assessment methodologies over the past 30 years, *ISET Journal of Earthquake Technology* **43**, 75–104.

Carausu, A., and Vulpe, A., 1996. Fragility estimation for seismically isolated nuclear structures by high confidence low probability of failure values and bilinear regression, *Nuclear Engineering and Design* **160**, 287–297.

Cornell, C. A., Jalayer, F., Hamburger, R. O., and Foutch, D. A., 2002. Probabilistic basis for 2000 SAC Federal Emergency Management Agency steel moment frame guidelines, *Journal of Structural Engineering* **128**, 526–533.

Cornell, C. A., and Krawinkler, H., 2000. Progress and challenges in seismic performance assessment, *PEER News* **3**.

Draper, N. R., and Smith, H., 1981. *Applied Regression Analysis*, 2nd edition, Wiley, New York, NY.

Eads, L., Miranda, E., Krawinkler, H., and Lignos, D. G., 2013. An efficient method for estimating the collapse risk of structures in seismic regions, *Earthquake Engineering and Structural Dynamics* **42**, 25–41.

Efron, B., and Tibshirani, R. J., 1993. *An Introduction to the Bootstrap, Monographs on Statistics & Applied Probability*, Chapman & Hall/CRC, Boca Raton, FL.

Ellingwood, B. R., and Kinali, K., 2009. Quantifying and communicating uncertainty in seismic risk assessment, *Structural Safety* **31**, 179–187.

Gehl, P., Seyedi, D. M., and Douglas, J., 2013. Vector-valued fragility functions for seismic risk evaluation, *Bulletin of Earthquake Engineering* **11**, 365–384.

Hancock, J., Bommer, J. J., and Stafford, P. J., 2008. Numbers of scaled and matched accelerograms required for inelastic dynamic analyses, *Earthquake Engineering and Structural Dynamics* **37**, 1585–1607.

Karim, K. R., and Yamazaki, F., 2003. A simplified method of constructing fragility curves for highway bridges, *Earthquake Engineering and Structural Dynamics* **32**, 1603–1626.

Kato, M., Takata, T., and Yamaguchi, A., 2008. Effective updating process of seismic fragilities using Bayesian method and information entropy, N6P1036, in *Proceedings of the Japan-Korean Symposium on Nuclear Thermal Hydraulics and Safety*, Okinawa, Japan.

Kennedy, R. P., Cornell, C. A., Campbell, R. D., Kaplan, S., and Perla, H. F., 1980. Probabilistic seismic safety study of an existing nuclear power plant, *Nuclear Engineering and Design* **59**, 315–338.

Kim, S. H., and Shinozuka, M., 2004. Development of fragility curves of bridges retrofitted by column jacketing, *Probabilistic Engineering Mechanics* **19**, 105–112.

Ku, H. H., 1966. Notes on the use of propagation of error formulas, *Journal of Research of the National Bureau of Standards – C. Engineering and Instrumentation* **70C**, 263–273.

Lestuzzi, P., Belmouden, Y., and Trueb, M., 2007. Non-linear seismic behavior of structures with limited hysteretic energy dissipation capacity, *Bulletin of Earthquake Engineering* **5**, 549–569.

Litton, R. W., 1975. A Contribution to the Analysis of Concrete Structures under Cyclic Loading, Ph.D. Thesis, Civil Engineering Dept., University of California, Berkeley.

Moehle, J., and Deierlein, G. G., 2004. A framework methodology for performance-based earthquake engineering, Paper No. 679, in *Proceedings of the 13th World Conference on Earthquake Engineering*, Vancouver, B.C., Canada.

National Institute of Building Sciences (NIBS), 2004. *HAZUS-MH: Users's Manual and Technical Manuals*, Federal Emergency Management Agency, Washington, D.C.

Otani, A., 1974. Inelastic analysis of R/C frame structures, *Journal of Structural Division* **100**, 1433–1449.

Pacific Earthquake Engineering Research Center (PEER), 2009. *Evaluation of Ground Motion Selection and Modification Methods: Predicting Median Interstory Drift Response of Buildings*, *PEER Report 2009/01* (C. B. Haselton, Ed.), PEER Ground Motion Selection and Modification Working Group, University of California, Berkeley, CA.

Porter, K., Kennedy, R., and Bachman, R., 2007. Creating fragility functions for performance-based earthquake engineering, *Earthquake Spectra* **23**, 471–489.

Pousse, G., Bonilla, L. F., Cotton, F., and Margerin, L., 2006. Non stationary stochastic simulation of strong ground motion time histories including natural variability: Application to the K-net Japanese database, *Bulletin of Seismological Society of America* **96**, 2103–2117.

Saez, E., Lopez-Caballero, F., and Modaressi-Farahman-Razavi, A., 2011. Effect of the inelastic dynamics soil-structure interaction on the seismic vulnerability assessment, *Structural Safety* **33**, 51–63.

Schwab, P., and Lestuzzi, P., 2007. Assessment of the seismic non-linear behaviour of ductile wall structures due to synthetics earthquakes, *Bulletin of Earthquake Engineering* **5**, 67–84.

Shinozuka, M., Feng, Q., Lee, J., and Naganuma, T., 2000. Statistical analysis of fragility curves, *Journal of Engineering Mechanics* **126**, 1224–1231.

Shome, N., and Cornell, C. A., 1999. *Probabilistic Seismic Demand Analysis of Nonlinear Structures*, *Tech. Rep. RMS–35*, RMS Program, Stanford University, Stanford, CA.

Shome, N., and Cornell, C. A., 2000. Structural seismic demand analysis: Consideration of "collapse," Paper No. 119, in *Proceedings of the 8th ASCE Specialty Conference on Probabilistic Mechanics and Structural Reliability*, ASCE, Reston, VA.

Shome, N., Cornell, C. A., Bazzurro, P., and Carballo, J. E., 1998. Earthquakes, records, and nonlinear responses, *Earthquake Spectra* **14**, 469–500.

Takeda, T., Sozen, M. A., and Nielsen, N. M., 1970. Reinforced concrete response to simulated earthquakes, *Journal of the Structural Division* **96**.

Vamvatsikos, D., and Cornell, C. A., 2002. Incremental dynamic analysis. *Earthquake Engineering and Structural Dynamics* **31**, 491–514.

Zentner, I., 2010. Numerical computation of fragility curves for NPP equipment, *Nuclear Engineering and Design* **240**, 1614–1621.

(Received 13 August 2012; accepted 10 June 2013)